ORIGINAL ARTICLE

CD109 regulates in vivo tumor invasion in lung adenocarcinoma through TGF-β signaling

Tetsuro Taki[1] [iD] | Yukihiro Shiraki[1,2] | Atsushi Enomoto[1] [iD] | Liang Weng[1] | Chen Chen[1] | Naoya Asai[3] | Yoshiki Murakumo[4] [iD] | Kohei Yokoi[5] | Masahide Takahashi[1,2] | Shinji Mii[1,2] [iD]

[1]Department of Pathology, Nagoya University Graduate School of Medicine, Nagoya, Japan

[2]Division of Molecular Pathology, Center for Neurological Disease and Cancer, Nagoya University Graduate School of Medicine, Nagoya, Japan

[3]Department of Molecular Pathology, Graduate School of Medicine, Fujita Health University, Toyoake, Japan

[4]Department of Pathology, Kitasato University School of Medicine, Sagamihara, Japan

[5]Department of Thoracic Surgery, Nagoya University Graduate School of Medicine, Nagoya, Japan

Correspondence
Masahide Takahashi and Shinji Mii, Department of Pathology, Nagoya University Graduate School of Medicine, 65 Tsurumai-cho, Showa-ku, Nagoya 466-8550, Japan.
mails: mtakaha@med.nagoya-u.ac.jp (M.T.); mii@med.nagoya-u.ac.jp (S.M.)

Funding information
Chukyo Longevity Medical and Promotion Foundation and Japan Society for the Promotion of Science (Grant/Award Number: "KAKENHI/19K07503," "KAKENHI/26221304").

Abstract

Stromal invasion is considered an important prognostic factor in patients with lung adenocarcinoma. The mechanisms underlying the formation of tumor stroma and stromal invasion have been studied in the lung; however, they are still unclear. CD109 is a glycosylphosphatidylinositol-anchored glycoprotein highly expressed in several types of human malignant tumors including lung cancers. In this study, we investigated the in vivo functions of CD109 protein in malignant lung tumors. Initially, we identified an association between higher expression of CD109 protein in human lung adenocarcinoma and a significantly worse prognosis, according to immunohistochemical analysis. We also showed that CD109 deficiency significantly reduced the area of stromal invasive lesions in a genetically engineered CD109-deficient lung adenocarcinoma mouse model, which correlated with the results observed in human lung adenocarcinoma. Furthermore, we identified latent TGF-β binding protein-1 (LTBP1) as a CD109-interacting protein using mass spectrometry and confirmed their interaction by co-immunoprecipitation. Importantly, increased CD109 expression enhanced stromal TGF-β activation in the presence of LTBP1. Therefore, these data suggest the significance of the regulation of TGF-β signaling through CD109 and LTBP1 interaction in tumor stroma and also reveal the importance of CD109 expression levels in promoting lung cancer cell proliferation, migration, and invasion, and thus predicting the outcome of patients suffering from lung adenocarcinoma. Therefore, CD109 protein could be a potential therapeutic target for this disease.

KEYWORDS
carcinogenesis, CD109, LTBP1, lung adenocarcinoma, mouse model

1 | INTRODUCTION

Lung cancer is the most common cause of cancer-related death worldwide, with adenocarcinoma accounting for half of all lung cancer cases.[1] Invasion is considered an important prognostic factor in patients with several cancers, including lung cancer. As the amount of normal stroma in lung is smaller than other organs, the mechanisms underlying the formation of tumor stroma and

stromal invasion have not been completely elucidated in lung adenocarcinoma.[2-4] In addition, lung adenocarcinoma is apparently heterogeneous, consisting of mixtures of histological subtypes and components, including some that are prognostically important.[5]

Recently, several animal models, such as $Kras^{LSL-G12D/+};p53^{flox/flox}$ mice (KP mice), have been developed to study human lung adenocarcinoma and for in vivo experiments.[6-8] Importantly, these genetically engineered tumor models exhibit tumor heterogeneity, stromal invasion, and metastasis, which are found in human carcinoma.[9] In addition, these mouse models have the advantage of presenting tumors in genetically normal lung tissue because of intratracheal random transfection of adenovirus.

CD109 is a glycosylphosphatidylinositol-anchored glycoprotein and a member of the α_2-macroglobulin/C3,C4,C5 family of thioester-containing proteins.[10,11] Although CD109 is a negative regulator of the transforming growth factor (TGF)-β signaling pathway in skin fibrosis[12,13] and skin squamous cell carcinoma,[14] the regulatory function of CD109 in TGF-β signaling is not yet fully understood in organs other than skin. Previous studies also reported CD109 expression in various malignant tumors[15-18] and its correlation with prognosis of patients harboring a malignant tumor such as lung adenocarcinoma.[18-21] However, precise in vivo functions of CD109 remain to be elucidated in malignant tumors. Additionally, CD109 may have a role in epidermal growth factor (EGF) signaling or phosphorylation of signal transducer and activator of transcription-3 (STAT3).[22]

In this study, we determined that CD109 deficiency significantly reduced stromal invasion and prolonged survival of the lung adenocarcinoma mouse model. Furthermore, we identified latent TGF-β binding protein-1 (LTBP1) as a CD109-interacting stromal protein, highlighting the significance of interaction between tumor cells and stroma in lung adenocarcinoma progression. These data also suggested that CD109 may have important roles not only in tumor cell–autonomous regulation but also in tumor-stromal interactions and that CD109 might be a potential therapeutic target for lung adenocarcinoma.

2 | MATERIALS AND METHODS

2.1 | Human lung adenocarcinoma samples

Surgically resected lung tissue samples from 200 lung adenocarcinoma patients, who provided informed consent, were obtained at Nagoya University Hospital from 2009 to 2011. This study was approved by the Ethics Committee of Nagoya University Graduate School of Medicine.

2.2 | Lung adenocarcinoma and $Cd109^{-/-}$ mouse models

In this study, we used KP mice as a lung adenocarcinoma mouse model,[9] which was generated by crossing $Kras^{LSL-G12D/+}$ and $p53^{flox/}$

^{flox} mice, both purchased from Jackson Laboratory (Bar Harbor, ME, USA). On the other hand, the generation of $Cd109^{-/-}$ mice and their characterization have been previously described.[23,24] Lung tumors were noted in 12- to 14-week-old KP mice at 28 days after intratracheal administration of adenoviral Cre recombinase (2.5×10^7 PFU), according to a previously described protocol.[9] Mice were sacrificed 12 weeks after tumor initiation for further examination. For survival analysis, the mice were euthanized when they presented respiratory distress. All experimental protocols were approved by the Nagoya University Animal Ethics Committee.

2.3 | Histological analysis

Human and mouse tissues were fixed in 10% neutral-buffered formalin, dehydrated, and embedded in paraffin. Immunohistochemical staining was performed as previously described.[23] The primary and secondary antibodies used in this analysis are indicated in Table S1. Two independent pathologists evaluated human tissues subjected to immunohistochemistry and stained with hematoxylin and eosin (H&E), Victoria blue-H&E, and Masson trichrome, as previously described.[3,6,18,25,26] The total immunostaining score of CD109 was calculated as the sum of a proportion score (PS) and an intensity score (IS). The PS reflects the estimated fraction of positively stained tumor cells (score 0, 0%-10%; score 1, 11%-30%; score 2, 31%-60%; score 3, 61%-100%). The intensity score represents the estimated staining intensity (score 0, negative; score 1, minimal; score 2, moderate; score 3, strong) giving a total score ranging from 0 to 6. We defined CD109-high as a total score > 3. ImageJ software (https://imagej.net/Fiji) was used to measure the number and area of tumor nodules and the area filled with α-smooth muscle actin (αSMA)-positive stromal cells in H&E and immunohistochemically stained mouse sections, respectively.

2.4 | Cell culture, transfection, and RNA interference

Human non–small cell lung cancer cell lines A431, A549, H1299, and H460 cells were purchased from American Type Culture Collection. Flp-In 293 cells were obtained from Thermo Fisher Scientific. WI-38 VA13 sub 2 RA was purchased from JCRB Cell Bank. All cell lines were maintained in DMEM or RPMI 1640 medium supplemented with 8% fetal bovine serum at 37°C in 5% CO_2. Two expression vectors, each one containing Flag- and HA-tagged CD109 (FH-CD109) sequences, were generated. Briefly, a cDNA fragment containing the CD109 full-length sequence with both Flag and HA tags was cloned after the signal peptide into both the pcDNA5/FRT (Thermo Fisher Scientific) and pRetroQ-AcGFP1-N1 plasmids (Takara Bio USA). FH-CD109-expressing Flp-In 293 (FH-CD109-293) and H1299 (FH-CD109-H1299) cells were generated using Flp-In system (Thermo Fisher Scientific) and retroviral-mediated gene transduction (Takara Bio USA), respectively, according to the manufacturers' instructions.

H460 cells were transiently transfected with LTBP1-expressing (H460-LTBP1) or empty pSV7d vectors (H460-VC). The pSV7d vectors were kindly provided by Kohei Miyazono (University of Tokyo). The sequences of siRNAs used in this study are described in "Supplementary methods."

2.5 | Generation of CD109 knockout cells using CRISPR/Cas9 genome editing

Two guide sequences were used for targeting human CD109 exon 2, #1:5′-CCCGGAGGAAATGTGACTAT-3′ or #2:5′-CCTCCGGGCCT GATGATCCC-3′. LentiCRISPRv2, pVSVg, and psPAX2 vectors (Addgene) were used to generate CRISPR/Cas9 lentivirus according to the manufacturer's protocol.[27]

2.6 | Western blot (WB) analysis

We followed a conventional protocol for WB analysis as previously described.[23] The primary and secondary antibodies used in this analysis are described in Table S2.

2.7 | Cell proliferation, migration, and invasion assays

Cell proliferation was measured using the water-soluble tetrazolium (WST)-1 assay (Roche). Directional cell migration of human cancer cells was stimulated in a monolayer using an in vitro scratch wound assay, as previously described.[28] The wound area was analyzed using ImageJ software and the filled wounded area was calculated as percentage of initial wound area. Cell invasion was evaluated in an organotypic culture model using immortalized cancer-associated fibroblasts (kindly provided by Takuya Kato) as previously described.[29]

2.8 | Co-immunoprecipitation (co-IP) assay and identification of CD109-interacting proteins

Cells were lysed in IP lysis buffer (50 mM Tris-HCl, 150 mM NaCl, 0.1% NP-40, 2 mM EDTA, pH 7.5) supplemented with cOmplete Mini Protease Inhibitor (Roche). The lysates were centrifuged at 12,000 g for 10 minutes at 4°C. The supernatants were incubated with 2 μg of the appropriate primary antibodies (Table S2) or normal IgG on a rotator at 4°C overnight, followed by the addition of 30 μL of anti-Flag M2 Agarose Affinity Gel or Protein G Sepharose, Fast Flow (Merck) at 4°C for 3 hours. Then, the beads were washed with IP lysis buffer, and the protein complex was eluted by boiling the sample with SDS sample buffer for 5 minutes.

For identification of CD109-interacting proteins, co-IP was performed by incubating the cell lysates with 20 μL of anti-Flag M2 Agarose Affinity Gel overnight at 4°C. Then, the beads were washed

with IP lysis buffer, followed by elution of the protein complex using 3 × Flag peptide (Merck). For the identification of proteins included in the eluate, the eluates were digested with Trypsin Gold (Promega) for 16 hours at 37°C, followed by analysis with Orbitrap Fusion Mass Spectrometer (Thermo Fisher Scientific).

2.9 | TGF-β bioassay

TGF-β activity was quantified with the luciferase[30] and secreted alkaline phosphatase (SEAP) detection assays.[31] Detailed protocols were described in Figure S1.

2.10 | Statistical analysis

In Kaplan-Meier analyses, differences between groups were evaluated by the log-rank test. For categorical variables, the chi-square test was performed. The independent t-test and Mann-Whitney U-test were used to compare sample means in a population with a normal and not normal distribution, respectively. Multivariate analysis was performed using a Cox proportional hazards model. A probability (P) value of ≤0.05 was considered significant using SPSS 25.0 (IBM) and GraphPad Prism 8 software (GraphPad Software). Data are expressed as the mean ± the standard deviations or standard error of the mean as indicated in the legends.

The methods used in the experiments for supplementary figures are described in Supplementary Document S1.

3 | RESULTS

3.1 | CD109 is expressed in lung adenocarcinomas

To examine the significance of CD109 protein in lung adenocarcinoma progression, we first examined the CD109 expression in lung adenocarcinoma by histological and immunohistochemical analyses. We detected CD109 expression in invasive lung adenocarcinoma, while it was not observed in noninvasive areas with lepidic pattern or adenocarcinoma in situ (Figure 1A). Especially, CD109 expression was detected at the invasive front into the tumor stroma (Figure S2).

This intriguing observation prompted us to analyze the expression of CD109 protein in adenocarcinoma samples of 200 patients by immunohistochemistry. In order to quantify the expression levels of CD109 protein, we defined a scoring system consisting of the CD109 staining intensity and the proportion of positive cells, and divided all cases into two groups: CD109-low and CD109-high, as described in Figure 1B. High CD109 expression was significantly correlated with invasive size (Figure 1C) and higher tumor grade (Figure 1D). Moreover, we determined that high CD109 expression was significantly correlated with a poor prognosis in all cases (Figure 1E) as well as in patients with T1 tumors (Figure 1F). CD109 expression was also significantly
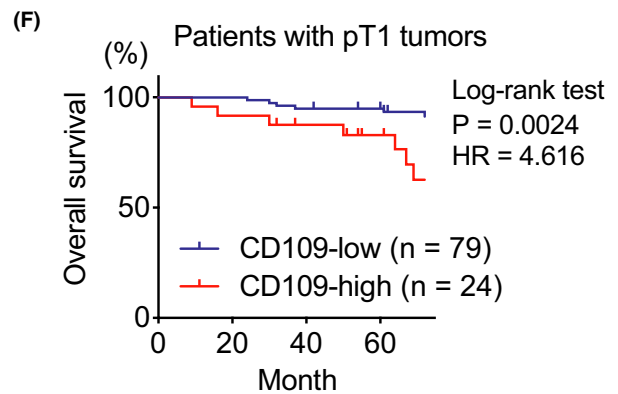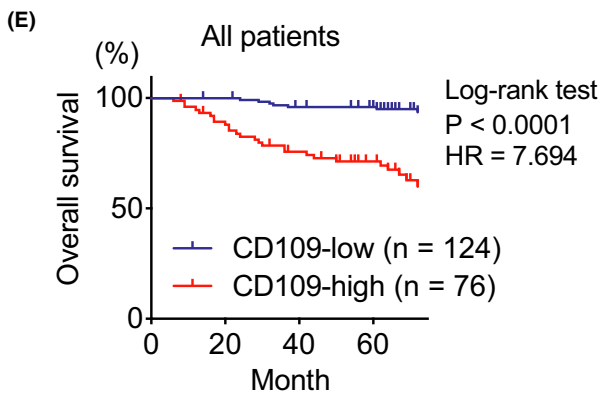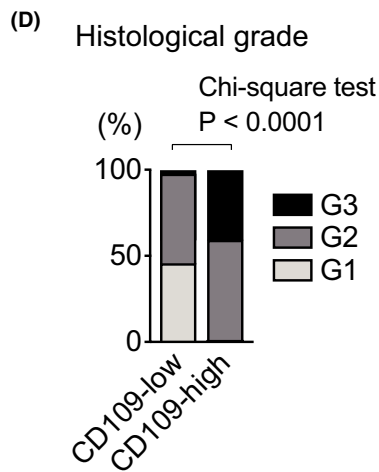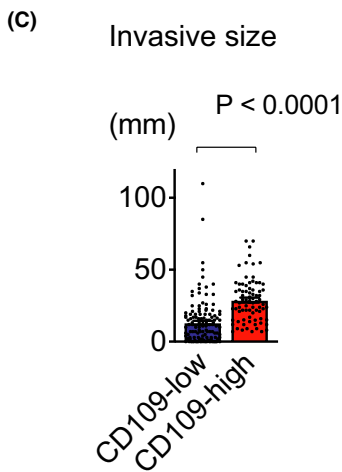
(A)

(B)

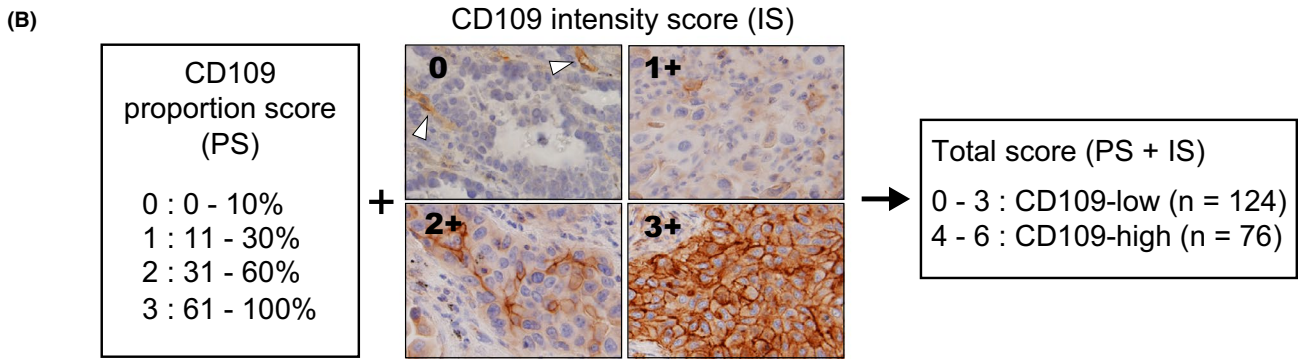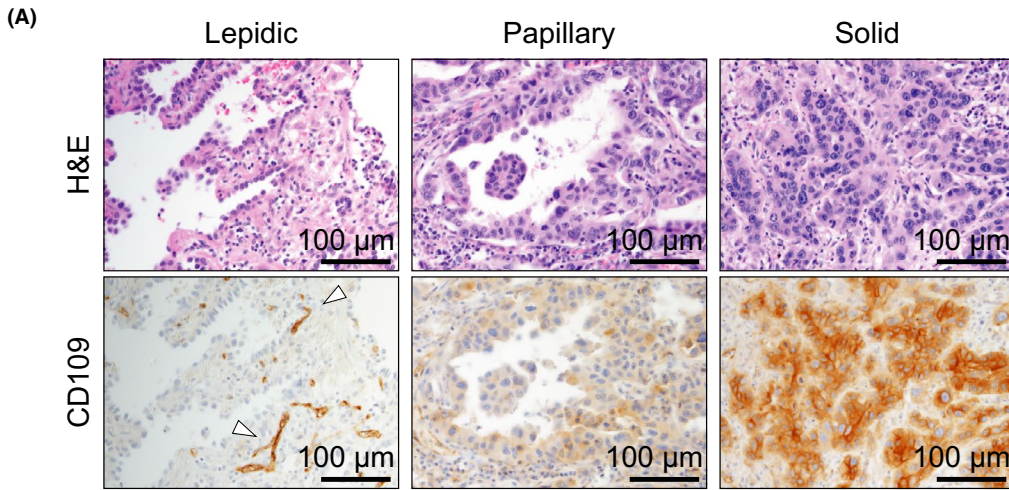**(C)**

(D)

(E)

(F)

FIGURE 1 CD109 protein expression correlates with tumor grade and prognosis in patients with lung adenocarcinomas. A, Representative histological images of human lung adenocarcinoma. H&E staining (upper panels) and immunohistochemical staining with anti-CD109 antibody (lower panels) in the same area in the serial section. B, The proportion score (PS) was assigned as follows: 0, 0%-10% tumor cells; 1, 11%-30% tumor cells; 2, 31%-60% tumor cells; 3, 61%-100% tumor cells. Representative images show each intensity score (IS). The intensity of CD109 staining was judged as 0-3+ (0, negative; 1+, minimal; 2+, moderate; 3+, strong) in tumor cells. The total score was calculated as the sum of PS and IS. Cases with total scores more than 3 were considered CD109-high. C, D, Invasive size (C) and histological grade (D) were determined in CD109-high (n = 76) and CD109-low (n = 124) tumors. E, F, Overall survival of the indicated group was analyzed by the Kaplan-Meier method in all patients (E) and patients with pT1 lung adenocarcinoma (F). Note that CD109-positive endothelial cells were observed in the representative images (arrowheads in A and B). Error bars indicate standard error of the mean. HR, hazard ratio

TABLE 1 Clinicopathological characteristics of lung adenocarcinoma patients

Characteristics	Total	CD109-low	(%)	CD109-high	(%)	χ^2 test P value
Number	200	124	(62.0)	76	(38.0)	
Age (y)						
<65	70	44	(22.0)	26	(13.0)	0.855
≥65	130	80	(40.0)	50	(25.0)	
Sex						
Male	106	48	(24.0)	58	(29.0)	<0.0001
Female	94	76	(38.0)	18	(9.0)	
Smoking history						
Never	90	70	(46.4)	20	(13.2)	0.0113
Smoked	61	35	(23.2)	26	(17.2)	
Unknown	49	19		30		
Pleural invasion						
(−)	152	113	(56.5)	39	(19.5)	<0.0001
(+)	48	11	(5.5)	37	(18.5)	
Lymphovascular infiltration						
(−)	163	117	(58.5)	46	(23.0)	<0.0001
(+)	37	7	(3.5)	30	(15.0)	
T classification						
Tis	25	25	(12.5)	0	(0.0)	<0.0001
T1	103	79	(39.5)	24	(12.0)	
T2	57	17	(8.5)	40	(20.0)	
T3 and 4	15	3	(1.5)	12	(6.0)	
N classification						
N0	175	119	(59.5)	56	(28.0)	<0.0001
N1, 2, and 3	25	5	(2.5)	20	(10.0)	
Clinical stage						
0	25	25	(12.5)	0	(0.0)	<0.0001
I	134	89	(44.5)	45	(22.5)	
II	23	4	(2.0)	19	(9.5)	
III	18	6	(3.0)	12	(6.0)	
EGFR mutation						
Nondetected	91	41	(24.1)	50	(29.4)	<0.0001
Detected	79	64	(37.6)	15	(8.8)	
Unknown	30	19		11		

TABLE 2 Univariate and multivariate analyses of prognostic parameters

	Univariate analysis			Multivariate analysis		
	P	RR	95% CI	*P*	RR	95% CI
CD109 (high)	<0.001	8.907	3.660-21.676	0.021	3.229	1.189-8.769
Clinical stage (II, III)	<0.001	6.709	3.327-13.527	0.001	4.004	1.750-9.162
Sex (Male)	0.587	1.213	0.603-2.440	–	–	–
Age (≥65)	0.707	0.872	0.426-1.783	–	–	–
EGFR mutation (detected)	0.005	0.250	0.094-0.663	0.158	0.481	0.174-1.329

Abbreviations: CI, confidence interval; RR, relative risk.

correlated with a poor prognosis in patients with or without mutations in epidermal growth factor receptor (EGFR) genes (Figure S3).

In Table 1, we summarized the clinicopathological features of these 200 patients, whose ages ranged from 26 to 84 years with a mean of 67.2 years. After univariate analysis, we performed multivariate analysis and revealed that CD109 expression and clinical stage were independent prognostic factors for overall survival, but not EGFR mutation (Table 2).

3.2 | CD109 deficiency reduces tumor invasion in a lung adenocarcinoma mouse model

Although the histological and immunohistochemical analyses suggested that CD109-positive tumor cells were preferentially observed at the invasive front of lung adenocarcinoma, this tendency was not clearly determined because of the intertumor diversity of human tumors. Therefore, we next continued this study by using a lung adenocarcinoma mouse model, which was generated by crossing $Kras^{LSL-G12D/+}$ mice with $p53^{flox/flox}$ mice and intratracheal administration of adenoviral Cre recombinase (KP mice; Figure 2A). We observed that lung tumors formed in $Cd109^{-/-}$ KP mice were apparently smaller than those in $Cd109^{+/+}$ KP mice, suggesting the involvement of CD109 in the progression of lung adenocarcinoma (Figure 2B and S4A,B). Average tumor burden, average tumor area, and the ratio of lung weight to body weight were significantly decreased in $Cd109^{-/-}$ mice compared with those in $Cd109^{+/+}$ KP mice (Figure 2C,D and S4C). More importantly,

H&E and Victoria blue-H&E stainings revealed that tumors in $Cd109^{+/+}$ mice include more disrupted elastic fibers than those in $Cd109^{-/-}$ mice (Figure 2E). We quantified the area of invasive lesions, namely, tumors with disrupted elastic fibers and found that the area was significantly increased in $Cd109^{+/+}$ mice compared with $Cd109^{-/-}$ mice (Figure 2F), while there was no significant difference in the total tumor number between $Cd109^{-/-}$ and $Cd109^{+/+}$ mice (Figure 2G). These data indicated that CD109 had an important role during in vivo tumor invasion. Histological analysis also showed that the tumor grade was significantly lower in $Cd109^{-/-}$ mice compared with that in $Cd109^{+/+}$ mice (Figure 2H,I). Vascular infiltration was observed in $Cd109^{+/+}$ mice (Figure S4D), as a difference to $Cd109^{-/-}$ mice. These histological findings were consistent with those observed in human lung adenocarcinoma (Figure 1D and Table 1). We also determined that CD109 deficiency was significantly correlated with a good prognosis in KP mice (Figure 2J).

3.3 | CD109 promotes cell proliferation, migration, and invasion of human lung cancer cells

We next investigated the function of CD109 using human lung adenocarcinoma cell lines. We generated CD109 knockout (CD109KO) A549 cells and FH-CD109-H1299 cells using the CRISPR/Cas9 system and retroviral-mediated gene transduction, respectively (Figure 3A,B). WST-1 assay revealed that cell proliferation was significantly decreased in CD109KO A549 cells and increased in FH-CD109-H1299 cells compared with their control cells, respectively

FIGURE 2 CD109 deficiency reduces tumor invasion in $Kras^{LSL-G12D/+}$;$p53^{flox/flox}$ (KP) mouse model. A, Schematic diagram of the carcinogenesis protocol in KP mice. B, Representative images of lungs (upper panels) and H&E-stained whole lung sections (lower panels) from $Cd109^{-/-}$ and $Cd109^{+/+}$ KP mice. C, Comparison of average tumor burden between $Cd109^{-/-}$ and $Cd109^{+/+}$ KP mice. D, Average tumor area in $Cd109^{-/-}$ and $Cd109^{+/+}$ KP mice. E, Representative histological images of elastic fibers in mouse lung adenocarcinomas at 12 wk after tumor initiation by adenovirus administration. H&E (upper panels) and Victoria blue-H&E (lower panels) stainings in the same area in the serial section. Left, noninvasive tumors with preserved elastic fibers in a $Cd109^{-/-}$ KP mouse. Right, invasive tumors with disrupted elastic fibers in a $Cd109^{+/+}$ KP mouse. F, The ratio of invasive lesion determined by Victoria blue staining to tumor area was expressed in percentage (n = 12 for $Cd109^{-/-}$ and n = 18 for $Cd109^{+/+}$ tumors). G, Tumor numbers in $Cd109^{-/-}$ (n = 12) and $Cd109^{+/+}$ (n = 18) KP mice. H, Representative histological images of $Cd109^{-/-}$ and $Cd109^{+/+}$ tumors for analysis of histological grade. I, Histological grade of the tumors in $Cd109^{-/-}$ and $Cd109^{+/+}$ KP mice using a previously described grading system.[6] For instance, histological grades of $Cd109^{-/-}$ and $Cd109^{+/+}$ tumors in (H) were determined as Grade 2 and 4, respectively. J, Survival rates of $Cd109^{-/-}$ (n = 11) and $Cd109^{+/+}$ (n = 10) KP mice were analyzed by the Kaplan-Meier method. Error bars indicate standard error of the mean. LW, lung weight; BW, body weight; HR, hazard ratio; n.s., not significant
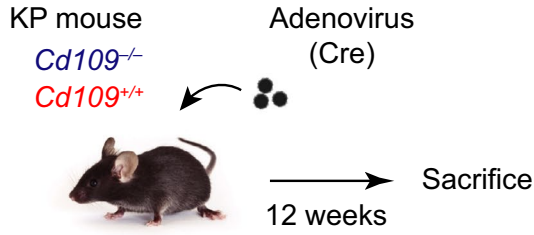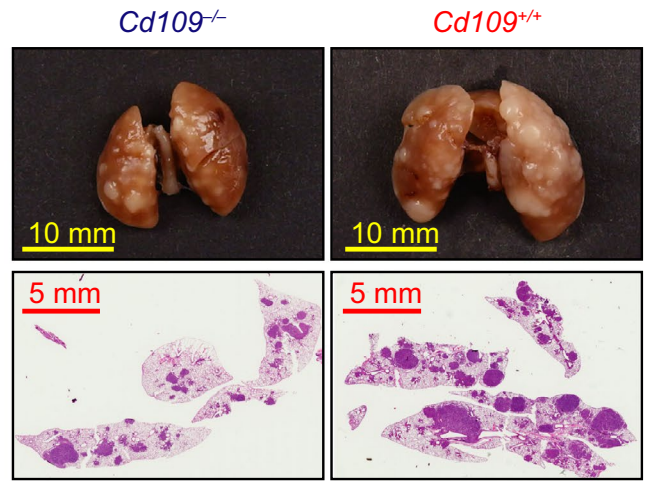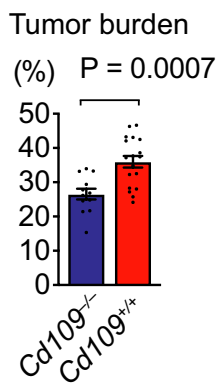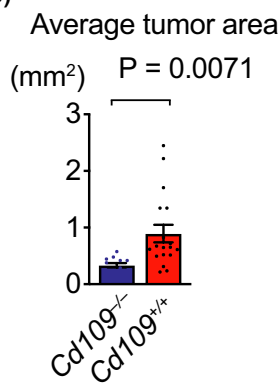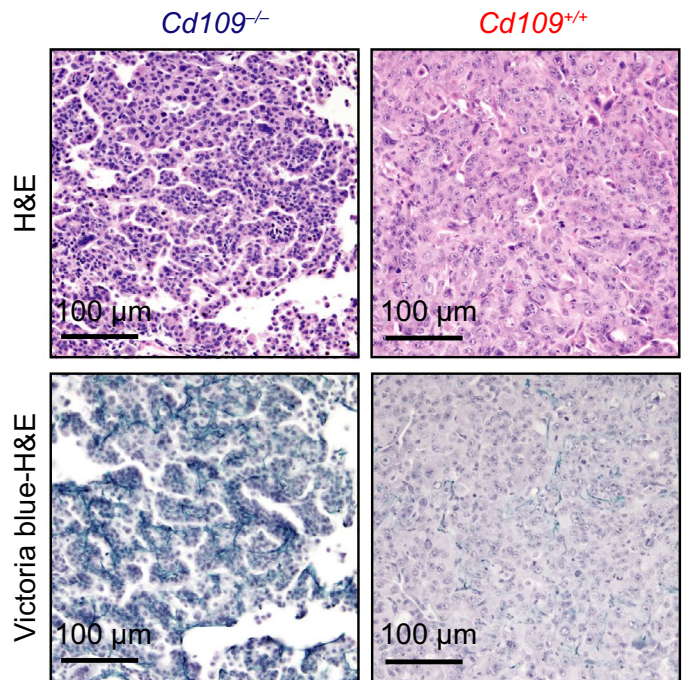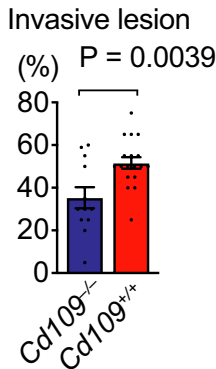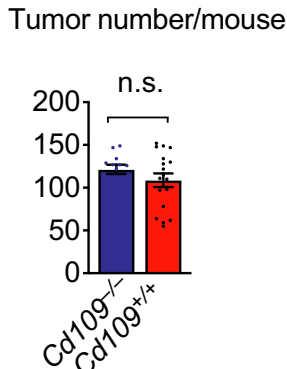
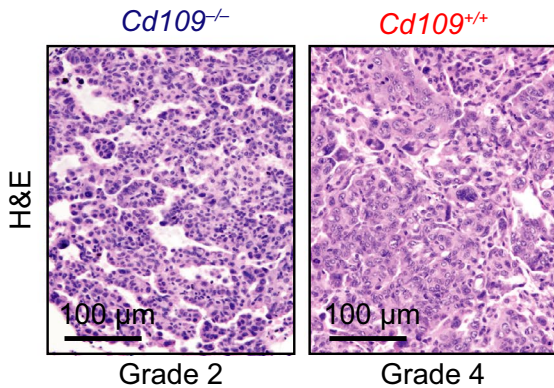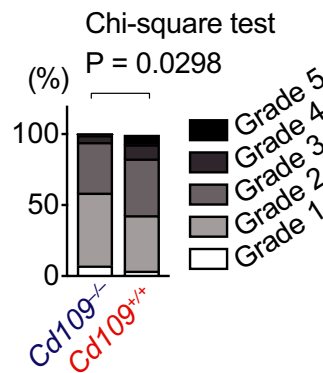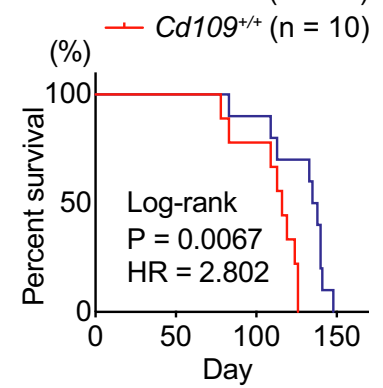(Figure 3C,D). In order to investigate whether CD109 expression altered cell migration, we performed in vitro wound healing assays. Cell migration, measured as filled wounded area, was significantly decreased in CD109KO A549 cells and increased in FH-CD109-H1299 cells compared with their control cells, respectively (Figure 3E,F). Moreover, cell invasion assay using an organotypic culture system demonstrated that FH-CD109 overexpression promoted cell invasion in H1299 cells compared with control FH-vector control (VC) cells (Figure 3G,H). These data suggested that CD109 protein promoted cell proliferation, migration, and tumor invasion in human lung adenocarcinoma.

Since CD109 is also known to have an important role in TGF-β signaling in skin keratinocytes[14,23] and EGF signaling in glioma cells,[32] we examined these signaling pathways by WB analyses. We did not detect apparent differences in the levels of phospho-Smad2 and phospho-EGFR proteins induced by TGF-β and EGF, respectively, between CD109KO and control cells (Figure S5A,B), while EGFR expression and phosphorylation were increased in FH-CD109-H1299 cells compared with control cells (Figure S5C). Gene Ontology (GO) enrichment analysis using DNA microarray data revealed that various GO terms including a GO term, negative regulation of cell proliferation (GO:0008285), were significantly enriched

in $Cd109^{-/-}$ lung tumors compared with $Cd109^{+/+}$ tumors (Table S3A). We also performed Q-PCR analysis to examine mRNA expression levels of $Ifng$, $Gata3$, and $Cdkn1a$ (p21) included in the GO term "negative regulation of cell proliferation" (Table S3B) and found that the expression of $Cdkn1a$ was significantly upregulated in $Cd109^{-/-}$ lung tumors compared with $Cd109^{+/+}$ tumors (Figure S5D). Furthermore, WB analysis using A549 cells showed that the expression level of p21 protein was increased in CD109KO cells compared with control cells (Figure S5E). On the other hand, no biological process related to epithelial to mesenchymal transition (EMT) was included in the list of enriched GO terms (Table S3A). Additionally, there was no apparent difference in the expression of proteins related to EMT between CD109KO and control A549 cells (Figure S5F) and between FH-CD109-H1299 and control cells (Figure S5G).

3.4 | CD109 is associated with fibrotic stromal reaction in human and mouse lung adenocarcinomas

The histological observation of invasive lung adenocarcinoma and the results of in vitro experiments including organotypic culture led us to further examine fibrotic stromal reaction, or scar, and stromal

FIGURE 3 CD109 promotes cell proliferation, migration, and invasion of human lung cancer cells. A, CD109KO A549 cells were generated using the CRISPR/Cas9 system. Expression of β-actin is shown as a loading control. B, Stable cell lines overexpressing FH-CD109 and FH-eGFP, as a control, were established using H1299 cells. Expression of β-actin is shown as a loading control. C, Cell proliferation in A549 cells was measured by WST-1 assay (n = 5). D, Cell proliferation in H1299 cells was measured by WST-1 assay (n = 4). E, In vitro wound healing assay using control (Ctrl LV) and CD109KO (#1, #2) A549 cells (n = 8). Percentage of wound area filled in 24 h was calculated as described in Section 2. F, In vitro wound healing assay using FH-eGFP- and FH-CD109-H1299 cells. Percentage of wound area filled in 8 h was calculated as given in (E) (n = 9). G, Representative H&E-stained images of Matrigel sections invaded by H1299 cells. H, The number of cell clusters invading the Matrigel was quantified in FH-CD109-H1299 and control (FH-VC) cells 10 days after initiation of culture (n = 4). Error bars indicate standard deviation. Ctrl, control; LV, lentivirus; FH-, Flag-HA-tagged; VC, vector control
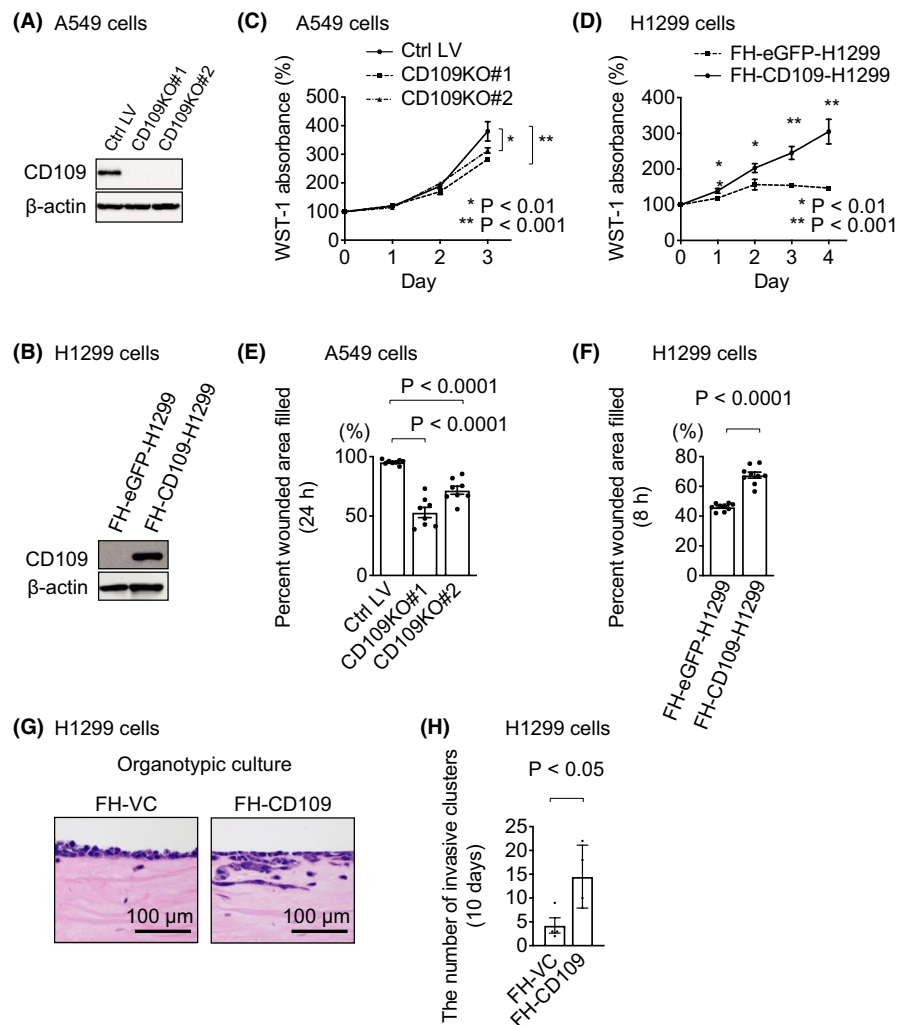
invasion in lung adenocarcinoma, which are important prognostic factors.[3,33] We determined the scar grade, a classification of fibrotic stromal reaction in human lung adenocarcinoma,[3] using Masson trichrome staining, which indicated collagenous stroma in blue (Figure 4A). The scar grade was significantly lower in the CD109-low group than in the CD109-high group (Figure 4B). We also examined fibrotic stromal reaction in mouse lung adenocarcinoma. Immunohistochemical analysis using an antibody against αSMA, a marker of activated fibroblasts (Figure 4C),[34] demonstrated that the percentage of αSMA-positive area was significantly smaller in *Cd109*$^{-/-}$ lung tumors than in *Cd109*$^{+/+}$ lung tumors (Figure 4D). These findings suggested that CD109 expression was associated with fibrotic stromal reaction in human and mouse lung adenocarcinomas.

3.5 | Screening of CD109-interacting proteins in a human lung adenocarcinoma cell line

Given the marginal differences in TGF-β and EGF signaling pathways between control and CD109-knockout or CD109-overexpressing cells (Figure S5A-C), the mechanisms underlying the poor prognosis and fibrotic stromal reaction of CD109-high lung adenocarcinoma remained elusive. In order to further elucidate this mechanism, we performed large-scale co-IP to isolate CD109-interacting proteins using lung adenocarcinoma cell line H1299 (FH-CD109-H1299) and Flp-In 293 (FH-CD109-293) cells (Figure 5A,B). The proteins isolated by co-IP were analyzed by mass spectrometry, and LTBP1 was detected in both cell lysates (Figure 5C and S6). We confirmed

endogenous LTBP-1 expression in H1299 and Flp-In 293 cells using WB analysis (Figure S7A,B). Furthermore, we performed reciprocal co-IP experiments using FH-CD109-293 and H460-LTBP1 cells, and confirmed the interaction not only between exogenous FH-CD109 and endogenous LTBP1 (Figure 5D,E) but also between endogenous CD109 and exogenous LTBP1 proteins (Figure 5F,G). On the other hand, interaction between CD109 and another candidate cell-surface protein, ADAM10 was not detected by co-IP using FH-CD109-293 cells (Figure S7C).

3.6 | CD109 modulates TGF-β signaling in tumor stroma through the interaction between CD109 and LTBP1

We performed a TGF-β bioassay using transfected mink lung epithelial cells (tMLECs), in which levels of luciferase and TGF-β activities were correlated, because this bioassay is a standard method to evaluate the effect of LTBP1 on TGF-β activation.[30] Before the bioassay, 293T cells were transiently transfected with TGF-β1-expressing and LTBP1-expressing vectors, followed by transient transfection with Flag-CD109-expressing or empty pcDNA3.1 + vector. The luciferase activity was significantly increased by the conditioned medium from 293T cells expressing Flag-CD109 (293T-CD109) compared with that from control cells transfected with empty vector (293T-VC) (Figure 6A). On the other hand, there was no significant difference in luciferase activity between the conditioned medium from 293T-CD109 and that from 293T-VC when both 293T cells were
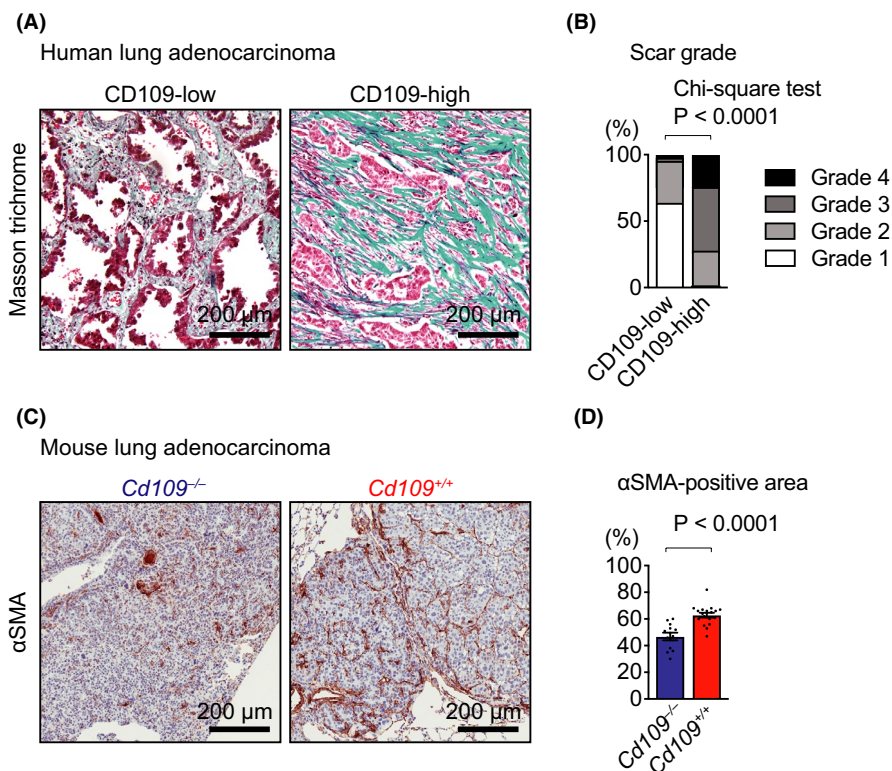

FIGURE 4 CD109 is associated with fibrotic stromal reaction in lung adenocarcinoma. A, Representative Masson's trichrome-stained images of collagenous stroma in CD109-low and CD109-high human lung adenocarcinomas. B, Correlation of CD109 expression with scar grades (n = 40 for CD109-low and n = 102 for CD109-high tumors). C, Representative images of fibrotic stromal reaction in tumors from *Kras*$^{LSL-G12D/+}$;*p53*$^{flox/flox}$ (KP) mice. Lung tumor sections were analyzed by immunohistochemistry using an antibody against αSMA, a marker of activated fibroblasts. D, The percentage of the area filled with αSMA-positive stromal cells in lung tumor area was measured in *Cd109*$^{-/-}$ (n = 12) and *Cd109*$^{+/+}$ (n = 18) KP mice. Error bars indicate standard error of the mean

FIGURE 5 Latent TGF-β binding protein (LTBP)-1 interacts with CD109 protein. A, B, Silver staining indicated the presence of CD109-interacting proteins, isolated by co-immunoprecipitation (co-IP) from FH-CD109-H1299 (A) and FH-CD109-293 (B) cell lysates. C, The proteins isolated by co-IP were analyzed by mass spectrometry. The numbers indicated in the Venn diagram are the numbers of the proteins whose scores were ten times higher in FH-CD109-expressing cells than in FH-eGFP control cells. D, E, FH-CD109-293 cell lysate was immunoprecipitated with anti-Flag affinity gel (D) or anti-LTBP1 antibody (E) and immunoblotted with indicated antibodies. F, G, H460-LTBP1 cell lysate was immunoprecipitated with anti-CD109 (F) or anti-LTBP1 (G) antibodies and immunoblotted with indicated antibodies. FH-eGFP-cell lysates were used as controls in (A-D). The closed and open red arrowheads in (D-G) indicate the position of LTBP1 and CD109 proteins, respectively. WI-38 and A431 cells were used as a positive and a negative control for LTBP1 expression in (D) and (F), respectively. Note that endogenous expression of LTBP1 was observed in Flp-In 293 ("Input" in D) and H460 ("H460-VC" in F) cells. FH-, Flag-HA-tagged; WI-38, WI-38 VA13 sub 2 RA; PC, positive control; NC, negative control; VC, vector control
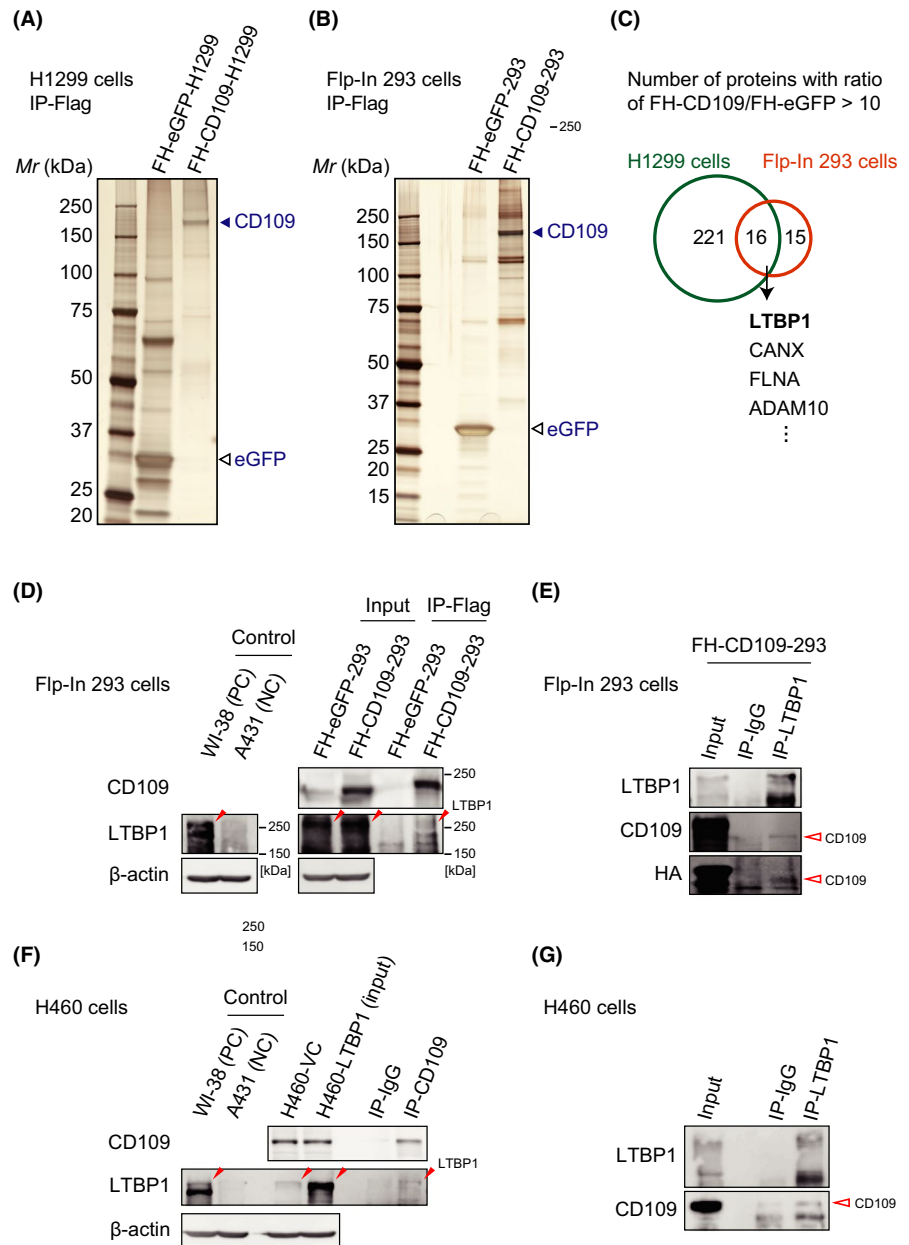
transfected with an empty vector instead of LTBP1-expressing vector (Figure 6B). Similar results were observed in the bioassay using FH-CD109-H1299 and FH-VC control cells (Figure S7D,E).

Additionally, we performed a SEAP detection assay using HEK-Blue TGF-β cells, in which SEAP and TGF-β activity levels were correlated. SEAP activity was significantly increased by the coculture of HEK-Blue TGF-β cells with FH-CD109-293 cells, compared with that of FH-VC-293 cells in the presence of TGF-β1 and LTBP1 (Figure 6C). On the other hand, there was no significant difference in SEAP activity between the coculture of HEK-Blue TGF-β cells with FH-CD109-293 and with FH-VC-293 cells lacking overexpression of LTBP1 (Figure 6D). These results indicated that CD109 interacted in vitro with LTBP1 and exerted a biological function. In addition, as the ELISA assay revealed that CD109 did not change the total TGF-β secretion in 293 cells (Figure S7F), CD109 may have an important role in TGF-β activation rather than in TGF-β secretion.

Furthermore, we confirmed in vivo TGF-β activity by immunohistochemical analysis. Immunohistochemical staining of CD109, LTBP1, and phospho-Smad2 (pSmad2) proteins in human lung adenocarcinoma revealed that the number of pSmad2-positive stromal cells was significantly increased in CD109-high (in cancer cells)/LTBP1-high (in stromal matrix) tumors as compared with the CD109-low/LTBP1-high tumors (Figure 6E,F).

We also performed in silico analysis using lung adenocarcinoma cases in a TCGA (The Cancer Genome Atlas) cohort. We classified them according to expression levels of *CD109* and *LTBP1* and analyzed the expression levels of genes related to fibrotic stromal reaction in cancer among the groups. Interestingly, their expression was significantly increased in the CD109-high/LTBP1-high group compared with that in the CD109-low/LTBP1-high group (Figure S8). This result was consistent with those of in vitro and in vivo experiments described above (Figure 6A-F).
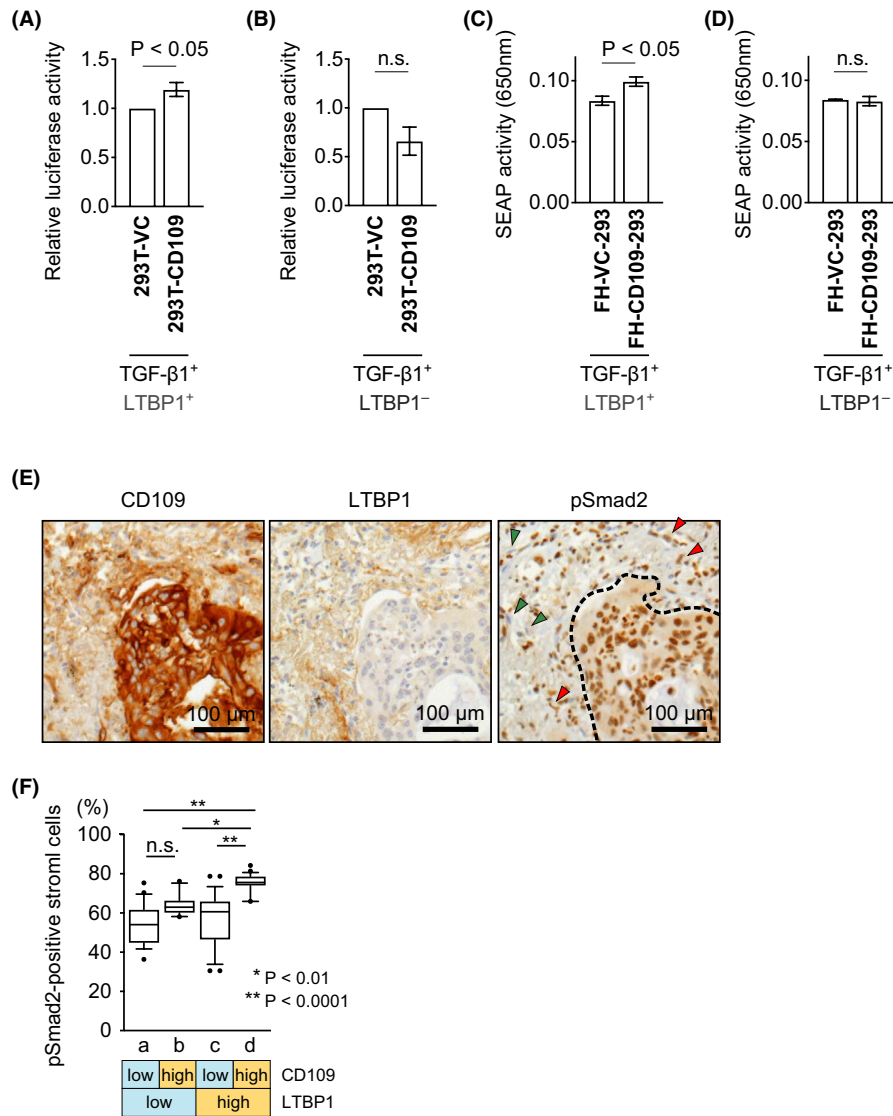
FIGURE 6 CD109 modulates TGF-β signaling by interacting with LTBP1. A, B, TGF-β bioassay with transfected mink lung epithelial cells (tMLEC) reporter cells using conditioned media from 293T cells transfected with Flag-CD109 expressing (293T-CD109) or empty vector (293T-VC). The 293T cells were previously transfected with TGF-β1-expressing vector and LTBP1-expressing (A) or empty vector (B). Luciferase activity was measured, and the ratio of Flag-CD109 expressing cells activity to that of control cells was calculated (A, n = 6; B, n = 4). C, D, HEK-Blue TGF-β cells were cocultured with Flp-In 293 cells stably expressing FH-CD109 (FH-CD109-293) or FH-VC (FH-VC-293), which were transiently transfected with TGF-β1-expressing vector and LTBP1-expressing (C) or empty vector (D) before coculture (n = 4). E, Representative images of immunohistochemical staining for CD109, LTBP1, and pSmad2 in human lung adenocarcinoma. Red and green arrowheads indicate pSmad2-positive and -negative stromal cells, respectively. Dotted line indicates the border between cancer cells and tumor stroma. F, Each HPF was classified into four groups (a, b, c, and d) according to CD109 and LTBP1 expression in cancer and tumor stromal cells, respectively, as indicated below the graph. The percentage of pSmad2-positive stromal cells were measured (n = 96 in total). Error bars indicate standard error of the mean in (A-D). Boxes represent the median and interquartile ranges for each group and whiskers show 10-90 percentiles in (F). VC, vector control; FH-, Flag-HA-tagged; SEAP, secreted alkaline phosphatase; n.s., not significant; HPF, high-power field

4 | DISCUSSION

In this study, we showed that the expression of CD109 protein was a prognostic marker of lung adenocarcinoma by using human tissue samples and the Kras-driven, p53-deficient lung adenocarcinoma mouse model (KP mice). Interestingly, we noted that CD109 deficiency significantly reduced the area of stromal invasive lesions in mouse lung adenocarcinoma, as observed in human lung

adenocarcinoma with lower CD109 expression. Therefore, these results, together with our cell invasion analysis showing that CD109 overexpression promoted cell invasion in lung adenocarcinoma cells, suggested that CD109 may have an important role in the interaction between tumor cells and stroma during lung adenocarcinoma progression.

A significant aspect of this study is that we used KP mice crossed with CD109-deficient mice. In general, human tumors have

intertumor genetic heterogeneity, which is affected by genetic or physiological conditions[35,36] and impedes the analysis of the disease. Our present study led to the provocative finding that CD109 protein was expressed in invasive components of human lung adenocarcinoma, while it was not observed in noninvasive areas. This result was supported by the analysis of *Cd109*^{+/+} and *Cd109*^{−/−} KP mice, which facilitated the histological analysis of genetically defined tumors.

It was recently reported that CD109 drove lung adenocarcinoma metastasis via a JAK/STAT signaling pathway.[21] We, however, observed that STAT3 phosphorylation was enhanced in CD109-deficient cells in the previous study.[23] These controversial results suggested that STAT3 phosphorylation was regulated by CD109 in a complicated manner depending on the cell and tissue contexts.[22] CD109 also played a role in EGF signaling in glioma cells,[32] which was often activated by mutant EGFR in lung adenocarcinoma.[37] In this study, there was no significant difference in EGFR phosphorylation between CD109KO and control cells. This finding, taken together with the result that CD109 expression constituted an independent prognostic factor in lung adenocarcinoma, suggested that CD109 was involved in lung adenocarcinoma progression, independently of its function in the EGF signaling pathway.

Also, LTBP1 was identified as a CD109-interacting protein in this study. LTBP1 is known as an extracellular matrix protein which mediates TGF-β signaling. LTBP1 forms a latent complex with TGF-β and latency-associated peptide. TGF-β is released from this complex by stimulation of integrins and other proteins to function in target cells.[38-40] Although LTBP1 expression is upregulated in malignant tumors, including glioma and ovarian cancers,[41,42] its function in tumors remains largely unknown. Our present finding of TGF-β activation in presence of CD109 and LTBP1 in TGF-β bioassays indicated that CD109 may play an important role in the modulatory effect of LTBP1 on stromal TGF-β signaling through its binding to LTBP1. Furthermore, our present immunohistochemical analysis showed an increase in the number of pSmad2-positive stromal cells in CD109-high/LTBP1-high tumors. Considering all these findings, we hypothesized that CD109-positive cells at the invasive front affected neighbor stromal cells that induced TGF-β activation through the interaction between CD109 and LTBP1 proteins. Reportedly, cancer microenvironment, including stromal fibrosis, is critical for tumor progression, metastasis, and resistance to treatments in various malignant tumors.[43,44] Stromal fibrosis is induced by the TGF-β signaling pathway in the tumor progression of various malignancies.[3,45-47] Therefore, it was noteworthy that CD109 expression was associated with stromal fibrosis represented by scar grade in lung adenocarcinoma. Our hypothesis was supported by a previous report showing that CD109 expression was increased in the fibrotic dermis of patients with systemic sclerosis.[13] Considering such CD109 function in nontumor tissue, we isolated CD109-interacting proteins using not only a cancer cell line H1299 but also a nontumor cell line 293. Although we found a novel upregulatory function of CD109 on TGF-β signaling, one potential limitation of our study is that we could not elucidate the relationship between this upregulating effect of CD109 on TGF-β signaling in tumor stroma and the downregulating effect of CD109

on epithelial cells, which was previously reported.[12,14,23,48,49] At present, the mechanisms underlying the paradoxical and context-dependent effects of TGF-β are still unclear.[13,22]

Furthermore, CD109 could be a potential therapeutic target because of its expression on the cell surface, enabling anti-CD109 antibodies to bind target cells in vivo, and because CD109-deficient mice exhibited no critical abnormalities.[23,24] Further investigation is required to develop in vivo CD109-targeting treatments.

DISCLOSURE

The authors have no conflict of interest.

ORCID

Tetsuro Taki 🔟 https://orcid.org/0000-0001-8654-6896
Atsushi Enomoto 🔟 https://orcid.org/0000-0002-9206-6116
Yoshiki Murakumo 🔟 https://orcid.org/0000-0003-2843-8189
Shinji Mii 🔟 https://orcid.org/0000-0001-8266-3235

REFERENCES

1. Travis WD, Brambilla E, Noguchi M, et al. International association for the study of lung cancer/American thoracic society/European respiratory society international multidisciplinary classification of lung adenocarcinoma. *J Thorac Oncol.* 2011;6:244-285.
2. Noguchi M, Morikawa A, Kawasaki M, et al. Small adenocarcinoma of the lung. Histologic characteristics and prognosis. *Cancer.* 1995;75:2844-2852.
3. Maeshima AM, Niki T, Maeshima A, et al. Modified scar grade: a prognostic indicator in small peripheral lung adenocarcinoma. *Cancer.* 2002;95:2546-2554.
4. Xi KX, Wen YS, Zhu CM, et al. Tumor-stroma ratio (TSR) in non-small cell lung cancer (NSCLC) patients after lung resection is a prognostic factor for survival. *J Thorac Dis.* 2017;9:4017-4026.
5. Travis WD, Brambilla E, Burke AP, et al. *WHO Classification of tumours of the lung, pleura, thymus and heart.* 4th ed. Lyon, France: IARC Press; 2015:26-37.
6. Jackson EL, Olive KP, Tuveson DA, et al. The differential effects of mutant p53 alleles on advanced murine lung cancer. *Cancer Res.* 2005;65:10280-10288.
7. Jackson EL, Willis N, Mercer K, et al. Analysis of lung tumor initiation and progression using conditional expression of oncogenic K-ras. *Genes Dev.* 2001;15:3243-3248.
8. Politi K, Zakowski MF, Fan PD, et al. Lung adenocarcinomas induced in mice by mutant EGF receptors found in human lung cancers respond to a tyrosine kinase inhibitor or to down-regulation of the receptors. *Genes Dev.* 2006;20:1496-1510.

9. DuPage M, Dooley AL, Jacks T. Conditional mouse lung cancer models using adenoviral or lentiviral delivery of Cre recombinase. *Nat Protoc*. 2009;4:1064-1072.

10. Lin M, Sutherland DR, Horsfall W, et al. Cell surface antigen CD109 is a novel member of the α_2 macroglobulin/C3, C4, C5 family of thioester-containing proteins. *Blood*. 2002;99:1683-1691.

11. Sutherland DR, Yeo E, Ryan A, et al. Identification of a cell-surface antigen associated with activated T lymphoblasts and activated platelets. *Blood*. 1991;77:84-93.

12. Litvinov IV, Bizet AA, Binamer Y, et al. CD109 release from the cell surface in human keratinocytes regulates TGF-β receptor expression, TGF-β signalling and STAT3 activation: relevance to psoriasis. *Exp Dermatol*. 2011;20:627-632.

13. Man XY, Finnson KW, Baron M, et al. CD109, a TGF-β co-receptor, attenuates extracellular matrix production in scleroderma skin fibroblasts. *Arthritis Res Ther*. 2012;14:R144.

14. Sunagawa M, Mii S, Enomoto A, et al. Suppression of skin tumorigenesis in CD109-deficient mice. *Oncotarget*. 2016;7:82836-82850.

15. Sato T, Murakumo Y, Hagiwara S, et al. High-level expression of CD109 is frequently detected in lung squamous cell carcinomas. *Pathol Int*. 2007;57:719-724.

16. Emori M, Tsukahara T, Murase M, et al. High expression of CD109 antigen regulates the phenotype of cancer stem-like cells/cancer-initiating cells in the novel epithelioid sarcoma cell line ESX and is related to poor prognosis of soft tissue sarcoma. *PLoS One*. 2013;8:e84187.

17. Tao J, Li H, Li Q, et al. CD109 is a potential target for triple-negative breast cancer. *Tumour Biol*. 2014;35:12083-12090.

18. Shiraki Y, Mii S, Enomoto A, et al. Significance of perivascular tumour cells defined by CD109 expression in progression of glioma. *J Pathol*. 2017;243:468-480.

19. Zhang F, Lin H, Gu A, et al. SWATH- and iTRAQ-based quantitative proteomic analyses reveal an overexpression and biological relevance of CD109 in advanced NSCLC. *J Proteomics*. 2014;102:125-136.

20. Shukla S, Evans JR, Malik R, et al. Development of a RNA-Seq based prognostic signature in lung adenocarcinoma. *J Natl Cancer Inst*. 2016;109:djw200.

21. Chuang CH, Greenside PG, Rogers ZN, et al. Molecular definition of a metastatic lung cancer state reveals a targetable CD109-Janus kinase-Stat axis. *Nat Med*. 2017;23:291-300.

22. Mii S, Enomoto A, Shiraki Y, et al. CD109: a multifunctional GPI-anchored protein with key roles in tumor progression and physiological homeostasis. *Pathol Int*. 2019;69:249-259.

23. Mii S, Murakumo Y, Asai N, et al. Epidermal hyperplasia and appendage abnormalities in mice lacking CD109. *Am J Pathol*. 2012;181:1180-1189.

24. Mii S, Hoshino A, Enomoto A, et al. CD109 deficiency induces osteopenia with an osteoporosis-like phenotype in vivo. *Genes Cells*. 2018;23:590-598.

25. Hagiwara S, Murakumo Y, Sato T, et al. Up-regulation of CD109 expression is associated with carcinogenesis of the squamous epithelium of the oral cavity. *Cancer Sci*. 2008;99:1916-1923.

26. Chen Y, Xing P, Chen Y, et al. High p-Smad2 expression in stromal fibroblasts predicts poor survival in patients with clinical stage I to IIIA non-small cell lung cancer. *World J Surg Oncol*. 2014;12:328.

27. Sanjana NE, Shalem O, Zhang F. Improved vectors and genome-wide libraries for CRISPR screening. *Nat Methods*. 2014;11:783-784.

28. Miyachi H, Mii S, Enomoto A, et al. Role of Girdin in intimal hyperplasia in vein grafts and efficacy of atelocollagen-mediated application of small interfering RNA for vein graft failure. *J Vasc Surg*. 2014;60:479-489.

29. Wang X, Enomoto A, Weng L, et al. Girdin/GIV regulates collective cancer cell migration by controlling cell adhesion and cytoskeletal organization. *Cancer Sci*. 2018;109:3643-3656.

30. Abe M, Harpel JG, Metz CN, et al. An assay for transforming growth factor-beta using cells transfected with a plasminogen activator inhibitor-1 promoter-luciferase construct. *Anal Biochem*. 1994;216:276-284.

31. Tesseur I, Zou K, Berber E, et al. Highly sensitive and specific bioassay for measuring bioactive TGF-β. *BMC Cell Biol*. 2006;7:15.

32. Zhang JM, Murakumo Y, Hagiwara S, et al. CD109 attenuates TGF-β1 signaling and enhances EGF signaling in SK-MG-1 human glioblastoma cells. *Biochem Biophys Res Commun*. 2015;459:252-258.

33. Eto T, Suzuki H, Honda A, et al. The changes of the stromal elastotic framework in the growth of peripheral lung adenocarcinomas. *Cancer*. 1996;77:646-656.

34. Gascard P, Tlsty TD. Carcinoma-associated fibroblasts: orchestrating the composition of malignancy. *Genes Dev*. 2016;30:1002-1019.

35. Jamal-Hanjani M, Quezada SA, Larkin J, et al. Translational implications of tumor heterogeneity. *Clin Cancer Res*. 2015;21:1258-1266.

36. Kim KT, Lee HW, Lee HO, et al. Single-cell mRNA sequencing identifies subclonal heterogeneity in anti-cancer drug responses of lung adenocarcinoma cells. *Genome Biol*. 2015;16:127.

37. Rikova K, Guo A, Zeng Q, et al. Global survey of phosphotyrosine signaling identifies oncogenic kinases in lung cancer. *Cell*. 2007;131:1190-1203.

38. Robertson IB, Horiguchi M, Zilberberg L, et al. Latent TGF-β-binding proteins. *Matrix Biol*. 2015;47:44-53.

39. Nunes I, Gleizes PE, Metz CN, et al. Latent transforming growth factor-beta binding protein domains involved in activation and transglutaminase-dependent cross-linking of latent transforming growth factor-beta. *J Cell Biol*. 1997;136:1151-1163.

40. Annes JP, Chen Y, Munger JS, et al. Integrin $\alpha_V\beta_6$-mediated activation of latent TGF-β requires the latent TGF-β binding protein-1. *J Cell Biol*. 2004;165:723-734.

41. Tritschler I, Gramatzki D, Capper D, et al. Modulation of TGF-β activity by latent TGF-β-binding protein 1 in human malignant glioma cells. *Int J Cancer*. 2009;125:530-540.

42. Higashi T, Sasagawa T, Inoue M, et al. Overexpression of latent transforming growth factor-β1 (TGF-β1) binding protein 1 (LTBP-1) in association with TGF-β1 in ovarian carcinoma. *Jpn J Cancer Res*. 2001;92:506-515.

43. Kalluri R. The biology and function of fibroblasts in cancer. *Nat Rev Cancer*. 2016;16:582-598.

44. Quail DF, Joyce JA. Microenvironmental regulation of tumor progression and metastasis. *Nat Med*. 2013;19:1423-1437.

45. de Kruijf EM, van Nes JG, van de Velde CJ, et al. Tumor-stroma ratio in the primary tumor is a prognostic factor in early breast cancer patients, especially in triple-negative carcinoma patients. *Breast Cancer Res Treat*. 2011;125:687-696.

46. Principe DR, DeCant B, Mascarinas E, et al. TGFβ signaling in the pancreatic tumor microenvironment promotes fibrosis and immune evasion to facilitate tumorigenesis. *Cancer Res*. 2016;76:2525-2539.

47. Wei Y, Kim TJ, Peng DH, et al. Fibroblast-specific inhibition of TGF-β1 signaling attenuates lung and tumor fibrosis. *J Clin Invest*. 2017;127:3675-3688.

48. Finnson KW, Tam BY, Liu K, et al. Identification of CD109 as part of the TGF-beta receptor system in human keratinocytes. *FASEB J*. 2006;20:1525-1527.

49. Hagiwara S, Murakumo Y, Mii S, et al. Processing of CD109 by furin and its role in the regulation of TGF-β signaling. *Oncogene*. 2010;29:2181-2191.

SUPPORTING INFORMATION

Additional supporting information may be found online in the Supporting Information section.